Check for updates

CrystEngComm

Accepted Manuscript

CrystEngComm

Volume 20
Number 15
21 April 2018
Pages 2071-2202

rsc.li/crystengcomm

PAPER
Yuan Zhuang et al.
Structural study on PVA assisted self-assembled 3D
hierarchical iron (hydr)oxides

ROYAL SOCIETY
OF CHEMISTRY
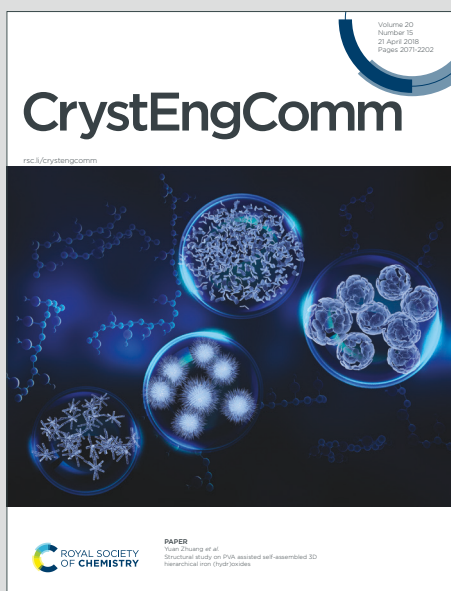
This is an Accepted Manuscript, which has been through the Royal Society of Chemistry peer review process and has been accepted for publication.

Accepted Manuscripts are published online shortly after acceptance, before technical editing, formatting and proof reading. Using this free service, authors can make their results available to the community, in citable form, before we publish the edited article. We will replace this Accepted Manuscript with the edited and formatted Advance Article as soon as it is available.

You can find more information about Accepted Manuscripts in the Information for Authors.

Please note that technical editing may introduce minor changes to the text and/or graphics, which may alter content. The journal's standard Terms & Conditions and the Ethical guidelines still apply. In no event shall the Royal Society of Chemistry be held responsible for any errors or omissions in this Accepted Manuscript or any consequences arising from the use of any information it contains.

ROYAL SOCIETY
OF CHEMISTRY

rsc.li/crystengcomm

ARTICLE

Structural, thermal and topological characterization of coordination networks containing flexible aminocarboxylate ligands with a central biphenylene scaffold

Davide Balestri,[a,c] Patrick Scilabra,[b] Claudia Carraro,[a] Andrea Delledonne,[a] Alessia Bacchi,[a,c] Paolo Pio Mazzeo[a,c] Lucia Carlucci,[d] and Paolo Pelagatti*,[a]
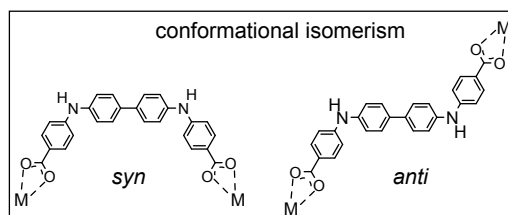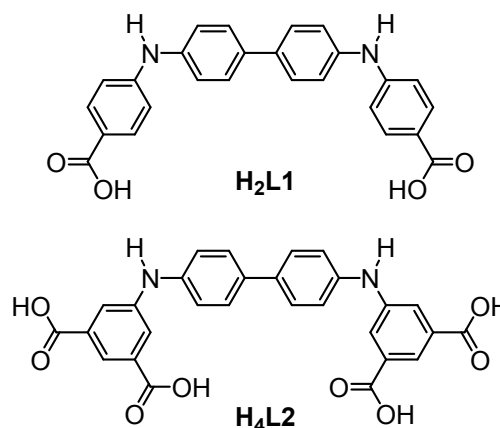
Four different coordination networks were isolated and structurally characterized by combining two aminocarboxylate ligands 4,4'-[Biphenyl-4,4'-diylbis(azanediyl)]dibenzoic acid and 5,5'-[Biphenyl-4,4'-diylbis(azanediyl)]diisophthalic acid (H$_2$L1 and H$_4$L2, respectively) with different transition metals (Zn(II), Zr(IV) and Cd(II)) under solvothermal conditions. The reaction between H$_2$L1 and Zn(NO$_3$)·6H$_2$O led to two different coordination networks. In PUMflex1-Zn, of formula {[Zn$_4$O(L1)$_3$(DMF)$_2$](DMF)$_4$}$_n$·(DMF)$_x$, the ligand displays always a *syn* conformation (with respect to the central biphenylene scaffold), while in the polymorph PUM*flex*1.1-Zn one of the three ligands composing the asymmetric unit adopts an *anti* conformation. Although the two supramolecular isomers have equivalent stoichiometry and dimensionality, they show different topology and entanglement type, that is parallel polycatenation of **6³-hcb** and 2-fold interpenetration of **4⁴-sql** layers, respectively. In the case of PUM*flex*1-Zr, of formula {[Zr$_6$O$_4$(OH)$_8$(L1)$_4$(H$_2$O)$_2$]$_n$·(DMF)$_x$, H$_2$L1 adopts and exclusive *syn* conformation, forming 1D-chains of rugby-ball shaped aggregates (topological type **2,8C1**) interconnected through H-bonds with water molecules. H$_4$L2 behaves instead as a dianionic ligand in PUM*flex*1-Cd, of ofrmula [Cd(κ²-COO)$_2$(DMF)$_3$(DMF)]$_n$, forming 1D zig-zag chains connected through N-H...O=C(OH) H-bonds to give planar layers of **sql** topology. In all cases the aptitude of the amine functions to interact with H-bond active guests is structurally highlighted by the recurrent N-H...O$_{DMF}$ interaction modelled in the X-ray structures.

Introduction

The use of polytopic aminocarboxylate ligands for the synthesis of coordination polymers is well documented in literature. For example, one of the aminocarboxylate ligands which has been widely investigated in its ability to create coordination networks is 4,4'-dicarboxy-diphenylamine, where a N-H function is introduced among two benzoate groups.[1–5] Curiously, the analogues tetratopic ligand 5,5'-azanediyldiisophthalic acid counts only a literature reported example, concerning a Cu-MOF.[6] The introduction of the amine group among the two aromatic rings interrupts the rigid Csp² skeleton, imparting to the ligand a V-shape. Continuing in our ongoing research program dealing with the use of N-H functionalized polytopic ligands containing a biphenylene scaffold,[7] we became interested in studying the self-assembly propensity of the ditopic ligands H$_2$L1 and H$_4$L2 towards transition metals (Scheme 1). H$_2$L1 is composed by two p-

benzoic acid end-groups spaced by a biphenylene scaffold bearing two N-H functions on positions 4 and 4'. H$_4$L2 bears instead two isophthalic acid end-groups, again spaced by two N-H functions on 4 and 4' position of a biphenylene scaffold. Hence, they can be considered extensions of 4,4'-dicarboxy-

a. Department of Chemical Sciences, Life Sciences and Environmental Sustainability, University of Parma, Parco Area delle Scienze 17/A, 43124 Parma, Italy.
b. Department of Chemistry, Materials and Chemistry Engineering "Giulio Natta", Politecnico di Milano, Via Mancinelli 7, 20131 Milano, Italy
c. Biopharmanet-TEC, Università degli studi di Parma, via Parco Area delle Scienze 27/A, 43124 Parma, Italy.
d. Department of Chemistry, Università degli Studi di Milano, via Golgi 19, 20133 Milano, Italy

ARTICLE

Scheme 1 Structure of ligands H2L1 and H4L2. Inset: the two possible conformations adopted by L1- during coordination.

diphenylamine and 5,5'-azanediyldiisophthalic acid ligands, respectively. Differently from these V-shaped ligands, H_2L1 and H_4L2 can adopt, during coordination, two different conformations, where the benzoate or isophthalate groups display a *syn* or *anti* conformation (see inset in Scheme 1 for H_2L1). This conformational isomerism augments the possible topologies reachable in the corresponding coordination polymers. Moreover, the N-H function results useful for

imparting host-guest propensity to the material, because of the possibility of creating H-bond contacts with incoming guest species. The two ligands were reacted with different transition metal ions under solvothermal conditions, and in this work we describe the solid-state structures of the frameworks obtained from the reactions between H_2L1 and $Zn(NO_3)_2$ or $ZrCl_4$, as well as the structure obtained reacting H_4L2 with $Cd(NO_3)_2$. The isolated frameworks highlight the versatile behaviour of the aminocarboxylate ligands towards the metal coordination, in terms of denticity and conformational isomerism. The thermal characterization of the new frameworks and their topological analysis are also reported.
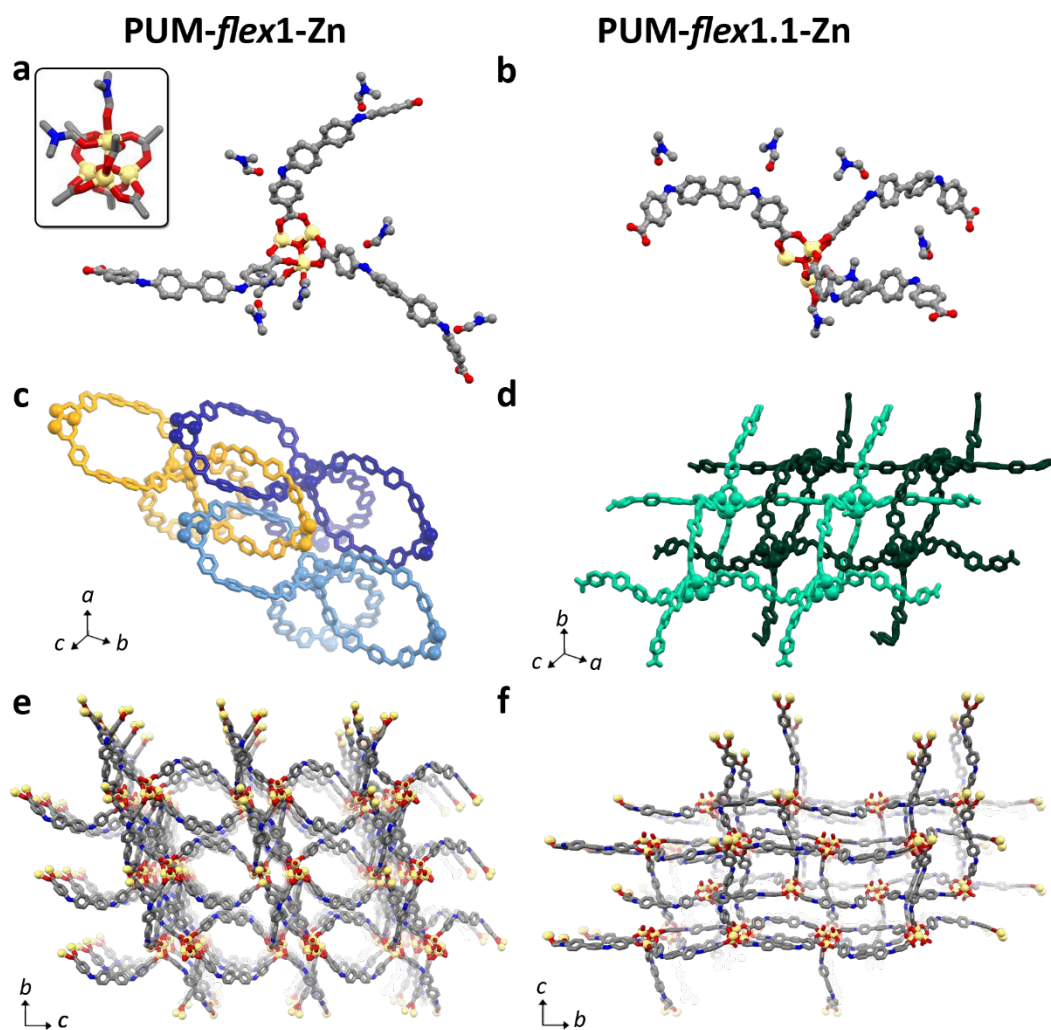
PUM-*flex*1-Zn   PUM-*flex*1.1-Zn

Figure 1 Crystallographic features of PUM*flex*1-Zn and PUM*flex*1.1-Zn: (inset) SBU found in both MOFs; a) asymmetric units for PUM*flex*1-Zn and b) PUM*flex*1.1-Zn; c) nets polycatenation for PUM*flex*1-Zn and d) nets interpenetration for PUM*flex*1.1-Zn, in both cases the coordinated DMF molecules have been omitted for the sake of clarity; e) views along axis a of the resulting architectures of PUM*flex*1-Zn and f) PUM*flex*1.1-Zn.

Results and discussion

The two ligands H_2L1 and H_4L2 are featured by different denticity and protic character. Hence, they can in principle give rise to coordination frameworks with different connectivity. The presence of the amine groups combined with the biphenyl scaffold makes possible different conformations, where the

two benzoate or isophthalate moieties can adopt a *syn* or *anti* mutual orientation (inset of Scheme 1). This feature enlarges the number of possible topologies that can be found in the isolated frameworks. The reaction between H_2L1 and $Zn(NO_3)_2 \cdot 6H_2O$ in DMF at 110°C led to the isolation of colourless plate-crystals, corresponding to PUM*flex*1-Zn (Figure S1). PUM stands for Parma University Materials. The structural analysis revealed that the crystal belongs to triclinic

space group *P-1*. As shown in Figure 1a, the asymmetric unit contains the tetrahedral O-centred cluster $Zn_4O(COO)_6$ (inset in Figure 1a), three L1^{2-} anions, two coordinated DMF molecules and four DMF molecules H-bonded to the amine N-H groups of the ligand (Figure 1a) (N…O distances ranging between 2.892 and 2.934 Å, N-H…O angles between 155° and 162°). This confirms the availability of the N-H groups to interact with hydrogen-bond acceptor guests.

In the SBU, the four Zn(II) ions are bridged by the oxide anion (μ^4-coordination), while each carboxylate group bridges two metal ions (κ^1:κ^1:μ^2-coordination). Three, out of the four Zn ions, display a tetrahedral coordination geometry, satisfied by the COO$^-$ groups belonging to three different L1^{2-} ligands, and by the μ^4-O^{2-} anion. The fourth Zn(II) ion displays an octahedral coordination geometry, completed by the COO groups of three L1^{2-} anions, the μ^4-O^{2-} anion and by two DMF molecules. As a whole, six L1^{2-} ligands depart from each SBU and each linker bridges two Zn(II) ions belonging to two different $Zn_4O(COO)_6$ tetrahedrons, allowing the expansion of the polymeric framework. The Zn…OOC distances are in the range 1.853-2.041 Å while the Zn…O$_{DMF}$ distances are in the range 2.030-2.112 Å, respectively. The Zn…(μ^4-O) distances are instead in the range 1.900-1.989 Å. All these values are comparable with those reported in the literature for similar SBUs.[8] The three independent dianion L1^{2-} adopt an almost exclusive *syn* conformation with torsion angles C$_{COO}$-N__N-C$_{COO}$ of 35.11°, 34.47 and -10.92°. The *syn* conformation combined with the bridging behaviour of L1^{2-} leads to the formation of the interconnected rings depicted in Figure 1c, whose approximate dimensions are 22.5x13.3 Å^2, measured considering the μ^4-O…μ^4-O and biphenyl…biphenyl distances, respectively. The combination between these metallamacrocycle motifs generates a 2D-planes (Figure S9).

The large void volume allows polycatenation: two additional sheets are interwoven to the first plane, generating a 3D infinite chainmail architecture, as shown in Figure 1c. The resulting architecture shows residual potential voids (3400 Å^3), corresponding to 44% of cell volume, after accounting for un-modelled electron density by the MASK procedure in Olex2.[9]

As evidenced by the residual un-modelled electron density (1120 electrons per unit cell, corresponding to 28 DMF molecules packed with 68% efficiency in the available volume), the cavities of the framework are certainly filled by heavily disordered solvent molecules, whose modelling was not possible. The remaining highest electron density residuals surround the metal atoms in the SBU hinting to a slight positional disorder of the entire framework, as observed in similar cases.[10] The formula of PUM*flex*1-Zn is then $\{[Zn_4O(L1)_3(DMF)_2](DMF)_4\}_n \cdot (DMF)_x$.

The available space in the MOF is made by cylindrical channels running along the a axis, with maximum dimensions of 17x14Å^2. Rectangular channels are instead visible along the b axis, with maximum dimensions of 21x15Å^2. (Figure S10) .

In one of the replicate syntheses of PUM*flex*1-Zn, beside the plate-like crystals, colourless rectangular prisms formed (Figure S2). The single crystal X-ray diffraction analysis revealed the formation of a new crystalline phase, hereinafter referred as PUM*flex*1.1-Zn. This crystallizes in the monoclinic space group $P2_1/n$. The structural analysis revealed that the new phase corresponds to a polymorphic framework of PUM*flex*1-Zn. The SBUs are equivalent, but one of the three independent L1^{2-} anion departing from each SBU adopts an *anti* conformation (torsion angles C$_{COO}$-N__N-C$_{COO}$ of -173.55°), while the other two adopt a *syn* or a slightly staggered conformation (torsion angle C$_{COO}$-N__N-C$_{COO}$ of 20.32° and -31.68°), as can be seen in Figure 1b. In this case the structure is 2D two-fold interpenetrated. Four DMF molecules, one disordered over two positions, hydrogen-bond to the amine functions were modelled indicating, once again, the receptor aptitude of this function (Figure 1b) (N…O ranging between 2.732 and 2.891 Å, N-H…O between 135 and 168°). The 2D-layers arrangement is very similar to the one seen in PUM*flex*1-Zn (Figure S11), but each ring is now interpenetrated only by one *anti*-ligand (Figure 1d and Figure S12). This packing motif results more efficient than the one found in PUM*flex*1-Zn, as evidenced by the reduced void volume corresponding to 3 cavities in the unit cell, one of V=2762 Å^3 and containing 630 electrons, the other two with V=541 Å^3 and 153 electrons, calculated after having removed all the unstructured electron density, and accounting for about 16 and 4 disordered DMF molecules, respectively. Repeated attempts aimed at reproducing PUM*flex*1.1-Zn as a pure phase failed, irrespective to the reaction temperature or ligand-to-metal molar ratio employed as well as the concentration of the reactant solution. In most of the cases PUM*flex*1-Zn was isolated as exclusive crystalline phase, while in others a mixture of the two phases formed. Unfortunately, the formation of PUM*flex*1.1-Zn appeared, in the end, neither reproducible nor predictable, showing a behaviour featuring disappearing polymorphs.

The solvothermal reaction between H$_2$L1 and ZrCl$_4$ in the presence of TFA as modulator led to PUM*flex*1-Zr. Crystals of PUM*flex*1-Zr were tiny needles which did not allow to collect good diffraction data, nevertheless it was possible to achieve a satisfactory structural determination to assess the architecture of the compound and to locate two water molecules firmly hydrogen bonded to two NH groups. The asymmetric unit contains one hexanuclear octahedral cluster of the type $[Zr_6(\mu^3\text{-O})_4(\mu^3\text{-OH})_4(OH)_4(COO)_8]$ (Figure 2a), four L1^{2-} anions and two lattice water molecules (Figure 2b). Each L1^{2-} anion bridges four Zr(IV) ions belonging to two different octahedral clusters, in a μ^4:κ^2:κ^2 mode. The Zr…OOC distances are in the range 1.74-2.50 Å, the Zr…OH distances are in the range 2.06-2.44 Å while the Zr…(μ^3-OH) or Zr…(μ^3-O) distances are in the range 1.90-2.45 Å. The Zr…Zr distances vary from 3.52 to 3.61Å. Each SBU is connected to two adjacent SBUs through eight L1^{2-} anions, developing chains running along b axis, as depicted in Figure 2c, which can be described as lines of rugby balls disposed along the main axle of the oval. The chain is then involved in hydrogen bonds with molecules of water contacting the amine moieties (O$_W$…H-N distances are in the range 2.04-2.25 Å). These contacts held together different chains (Figure 2d) building a 3D network which exhibits open square channels of 14x14 Å^2, along crystallographic axis b

(Figure 2e). The calculated void volume is 57% of unit cell (5267 $\mathring{A}^3$), after removal of the residual electron density (1285 electrons, corresponding to about 30 loosely packed DMF molecules). The formula of PUM*flex*1-Zr is then $\{[Zr_6O_4(OH)_8(L1)_4(H_2O)_2]_n\}\cdot(DMF)_x$.
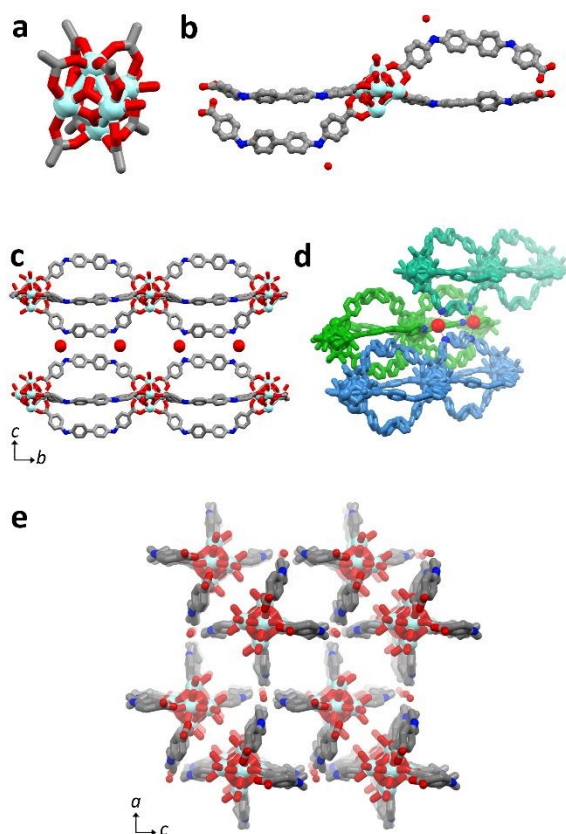
Figure 2 Structural features of PUM*flex*1-Zr: a) Octahedral SBU; b) Asymmetric unit with the molecules of water represented as red spheres; c) chains of rugby ball shaped assemblies along a axis; d) 3D network composed by rugby-ball lines hydrogen bonded to water molecules, represented by red spheres; e) view of the square channels along crystallographic axis b.

The solvothermal reaction between H_4L2 and $Cd(NO_3)_2 \cdot 4H_2O$ led to the isolation of light-yellow plate-crystals of PUM*flex*2-Cd. The asymmetric unit contains a Cd(II) ion, one H_2L2^{2-} dianion, and three coordinated molecules of DMF (each one disordered over two orientations) (Figures 3b and S17). A further half occupied DMF molecule disordered over two positions is found in the structure. Cd is seven-coordinate being surrounded by four carboxylate oxygens and three DMF oxygens and the SBU formula is $[Cd(\kappa^2\text{-}COO)_2(DMF)_3]$ (Figure 3a). The Cd-OOC distances are in the range 2.360-2.370Å, the Cd-O_{DMF} distances are in the range 2.276-2.287Å. The dianion H_2L2^{2-} adopts an *anti*-conformation. Despite the tetratopic character, the aminocarboxylate linker acts as bidentate ligand using two centrosymmetrically related carboxylate functions to bind two metal ions, forming infinite 1D zig-zag chains with Cd…Cd distances of 18.665Å (Figure 3c). The chains are slightly shifted one with respect to the other, and this shift places the NH and COOH groups of two linkers belonging to two adjacent chains in the correct orientation to form two $R_2^2(14)$ supramolecular rings, based on Etter notation.[11] To remove steric hindrance, the biphenyl scaffold rotates around the N-C bond in such a way to form, with the isophthalate plane, a dihedral angle of 36.3°. These N-H…O hydrogen bonds connect

the 1D chains forming a 2D supramolecular network. Moreover, the COOH groups of the aminocarboxylate linker behave as H-bond donor towards the coordinated COO moiety of a linker belonging to a neighbouring chain (COOH…OOC distance of 2.55Å with an angle of 163°), developing the whole framework in the third dimension (Figure 3d). The resulting supramolecular architecture shows channels running along crystallographic axis b. However, the coordinated DMF molecules occlude almost completely the channels creating chambers (Figure 3e). In fact, the framework leaves four voids *per* cell each with a free volume of 180Å³, which is occupied by a disordered DMF molecule, located in the electron density map and modelled over two positions. The formula of PUM*flex*2-Cd is then $\{[Cd(H_2L2)(DMF)_3](DMF)\}_n$.
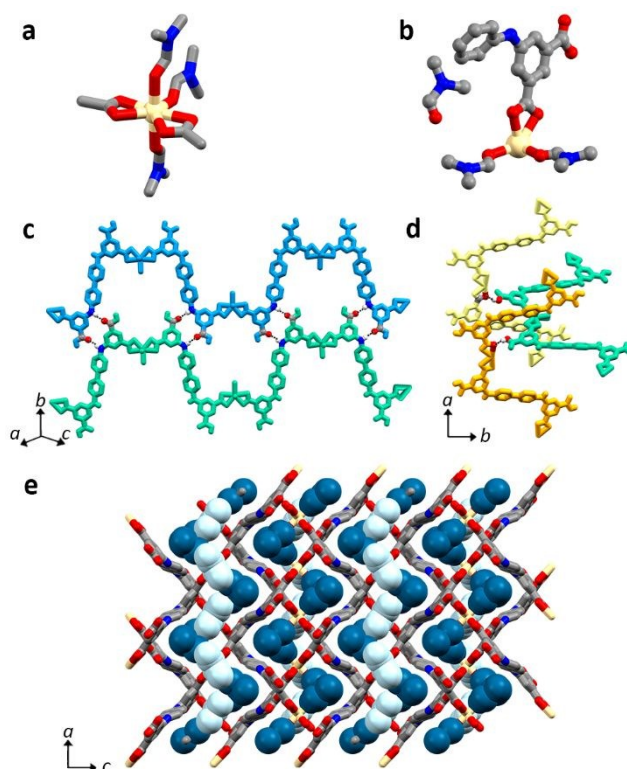

Figure 3 Crystallographic features of PUM*flex*2-Cd: a) SBU structure; b) asymmetric unit; c) H-bond contacts between zig-zag chains involving COOH and NH groups giving a 2D-supramolecular layer; d) COOH…COO contacts between adjacent chains; e) view along axis b of the overall 3D supramolecular architecture (DMF molecules are plotted in spacefill style, light blue colour for the DMF molecules lying on the carboxylate plane, dark blue colour for the two Cd-coordinated DMF molecules).

Thermal characterization

Loss of the included DMF molecules led to extensive degradation of the crystals of PUM*flex*1-Zn and PUM*flex*1.1-Zn, as seen storing the crystals at room temperature on the laboratory bench. This is imputable to the loss of loosely bound solvent molecules and has a negative impact on the elemental analyses results. However, DMF thermal extrusion can be evidenced by TGA analysis. As expected, the thermal profiles of the two polymorphs are similar. The framework of PUM*flex*1-Zn shows an excellent thermal stability, as evidenced by TGA analysis, with decomposition occurring at

ARTICLE

T>380°C. The decomposition is preceded by a 22% weight decrease, corresponding to the loss of 6 DMF molecules (Figure S18), in agreement with those modelled in the structural characterization. The DMF departure occurs by two weight losses in the T-intervals 80-152 °C and 153-232 °C, corresponding to 15.3% (4 molecules of DMF, assumed to be those H-bonded to the amide groups) and 6.7% (2 molecules of DMF, assumed to be those coordinated to Zn) weight loss percentage, respectively. The result indicates that all the unmodelled DMF molecules are lost during storage of the sample, justifying the observed degradation of the crystals.

The TGA trace of PUM*flex*1.1-Zn shows a loss weight percentage of 33%, prior to decompose at a temperature higher than 400 °C (Figure S19). The weight loss percentage corresponds to the departure of a number of DMF molecules higher than the one structurally modelled (9 vs 6). This means that, contrarily to PUM*flex*1-Zn, part of the unmodelled DMF molecules are retained during storage, in agreement with the reduced void volume found in PUM*flex*1.1-Zn. Also in this case the solvent loss occurs in two steps. The first ends within 140 °C, while the second occurs between 140 °C to 220 °C. Also in this case the second step corresponds to 2 molecules of DMF, which are assumed to be those directly bound to the metal. The thermal decomposition of PUM*flex*1-Zr occurs around 380°C. The thermal curve (Figure S20) shows a mass loss of 22% in the range 117-260 °C, attributed to the departure of 7 DMF molecules and the two H-bonded water molecules. A second smaller loss corresponding to 8.25% weight percentage is then observed in the T-interval 261-366 °C. These last values are similar to those described by Cavka et al.[12] for the dihydroxylation of the cluster $Zr_6O_4(OH)_4(RCOO)_{12}$ to $Zr_6O_8(RCOO)_{12}$, occurring in the T-interval 250-300 °C. FTIR analysis conducted on a sample of PUM*flex*1-Zr after thermal treatment at 350 °C shows the disappearance of the broad band in the region 2700-3500 cm^{-1} (OH region), indicating dihydroxylation of the Zr-cluster (Figures S23-24). The band relative to the N-H stretching is instead still present. In the region 1700-1500 cm^{-1} the disappearance of the band centred at 1652 cm^{-1} is indicative of the DMF departure. The other bands remain unchanged to indicate the integrity of ligand L1. Thermal decomposition of PUM*flex*2-Cd occurs instead at T>330°C, preceded by an extended desolvation step in the T-interval 95-225°C (Figure S21), corresponding to 30% weight loss. This data is in perfect agreement with the departure of the DMF molecules structurally found.

Topological analysis

The topology and entanglement of the assembled networks is affected by the long and flexible nature of the used bis-carboxylate ligands, which easily give rings trough *syn* conformation, and by their ability to give hydrogen bonds.

From a topological point of view PUM*flex*1-Zn can be described as a 2D coordination network of 6^3-**hcb** topology where the 3-connected nodes (3-c) are the $Zn_4O(COO)_6$ units and all the six edges of the hexagonal windows are bridged by two carboxylate ligands (see Figure 4a). The 2D network shows, therefore, the feature to have all edges as 2-loops. The

layers, which have a thickness of ca. 9.21 Å and are all (2 1 1) oriented, are parallel polycatenated giving a 2D→3D array. In the entangled 3D array each layer is catenated to two other layers, one above and one below, while it is necessary to remove one layer to separate the whole 3D array in two parts, so that Doc=2 and IS=1. 2D networks of **hcb** topology where all edges are 2-loops are not common, moreover, the entanglement in PUM*flex*1-Zn shows peculiar and interesting features. Not all rings are involved in the catenation and only 2/3 of the 2-loops of one hexagonal window (that is, four of six) are utilized in the catenation. Each of these are crossed by two rings belonging to the two adjacent layers, respectively, above and below while the other two are free (see Figure 4b). The polycatenation in *PUMflex*1-Zn occurs through Hopf-links which is quite unusual in the entanglement of 2D motifs

Figure 4: Polycatenation in PUM*flex*1-Zn: a) View of a single **hcb** layer evidencing the 2-loop edges; b) entanglement of a single hexagonal window with the layer above and
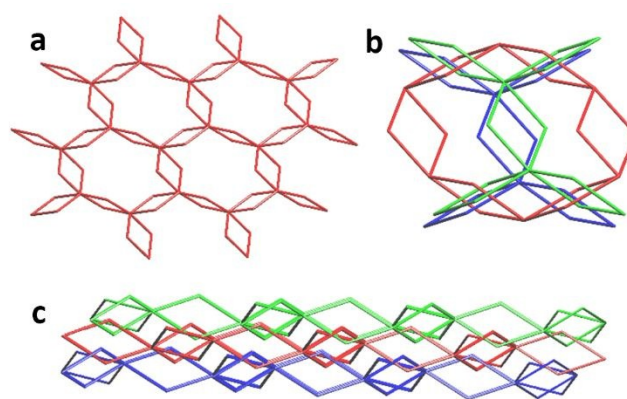
below; c) a lateral view showing the parallel polycatenation of 3 layers.

containing 2-loops where the rotaxane type link is more usual.[13-15]

To the best of our knowledge,[16] only one structure (CSD refcode: NAKREZ)[17] is reported showing parallel polycatenation (Figure 4c) trough Hopf-links of 2D layers of **hcb** topology where all edges are 2-loops. In NAKREZ, however, all loops are involved in the polycatenation even if two of six are double crossed and four of six are single crossed. PUM*flex*1.1-Zn is a 2D coordination network parallel to the (1 0 -1) plane which can be simplified to 4^4-**sql** topology in which the 4-c nodes are the $Zn_4O(COO)_6$ units and the two opposite edges of the square windows are 2-loops (Figure 5a). This motif, among entangled 2D networks with 2-loops, is more common than the previous one.[13-15] Here the 2D layers show 2-fold interpenetration through rotaxane-like link. All 2-loops of one layer are threaded by the single edges of the second one giving an entanglement described by a rotaxane of 1.1 type (one ring one axle).

Simplification of PUM*flex*1-Zr gives 1D chains of 2,8C1 topological type in which the Zr clusters behave as 8-c nodes which are bridged by four ligands (Figure 5b). A search in the ToposPro[18] database gives 17 examples (see Table S1) for complete list) of 1D coordination chains of the same topological type. These, however, are all of lanthanide metals and the bridging ligands are carboxylates, apart few examples. PUM*flex*1-Zr is, thus, unique given the nature of the 8-c Zr-cluster nodes and the long flexible bridging carboxylate ligands. The chains running parallel to the *b* direction are all connected each other by hydrogen bonds between N-H and water molecules to give a multinodal complex 3D network.
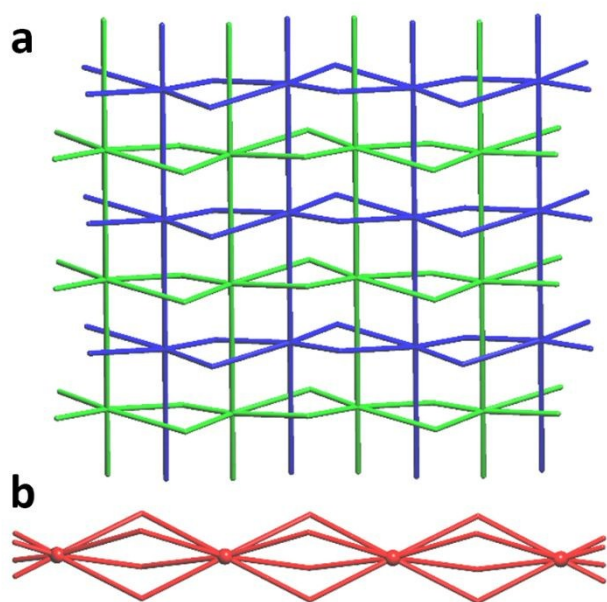

Figure 5 a) View of the simplified 2-fold interpenetrated **sql** layers in PUM*flex*1.1-Zn; b) View of the simplified 2,8C1 chain in PUM*flex*1-Zr.

In PUM*flex*1-Cd the 1D zig-zag chains run along the [2 0 1] and [2 0 -1] directions giving two sets of parallel chains. Within each set the chains are slightly shifted and connected by the $R_2^2(14)$ hydrogen bonds to give two sets of flat supramolecular layers of **sql** topology (Figure 6a) parallel to (1,0,-2) and (1,0,2) planes, respectively. Interestingly, the two sets of layers, which make an angle of 81.1°, give a 3D supramolecular array by inclined polycatenation. Each window of a layer is catenated with two windows of two different layers belonging to the inclined set of layers, so that, the density of catenation is Doc = 2/2 (Figure 6b). The short COOH…OOC hydrogen bonds further connect the two sets of polycatenated layers to give a single multinodal self-penetrate 3D supramolecular framework.
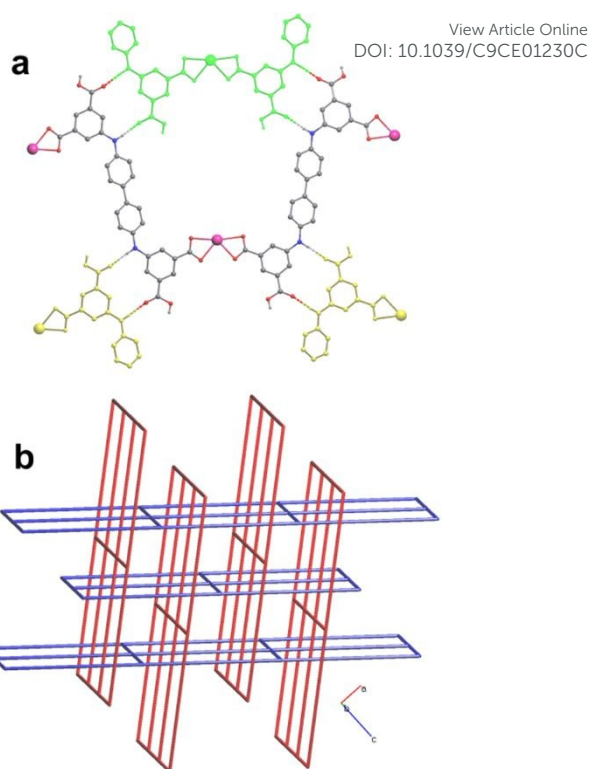
Experimental

Figure 6 a) View of a square window of the **sql** layer in PUM*flex*1-Cd built by R_2^2 (14) hydrogen bonds between coplanar zig-zag chains (shown in different color); b) Simplified view of the inclined polycatenated array in PUM*flex*1-Cd.

Materials and methods

All chemicals and solvents were purchased by commercial suppliers and used as received. Ligands H_2L1 and H_4L2 were synthesized as previously reported.[19] Crystalline materials PUM*flex*1-Zn, PUM*flex*1-Zr and PUM*flex*2-Cd were synthesized using solvothermal conditions. ^1H NMR spectra were recorded on a Bruker Avance 300 MHz or 400 MHz instruments. Chemical shifts are reported in ppm relative to the solvent residual peak of $(CD_3)_2SO$ (δH 2.50, δC 39.5). IR spectra were obtained with a Thermo Scientific Nicolet 5PCFT-IR-ATR spectrometer (diamond crystal) in the 4000-400cm^{-1} interval. Thermogravimetric analyses were performed on a PerkinElmer 8000 instrument (sample mass approx. 5-10 mg) at a heating rate of 10 °C min^{-1} in a temperature range from 25-500 °C. The measurement was performed at atmospheric pressure under flowing nitrogen (80 mL min^{-1}).

Synthetic procedures

The ligands H_2L1 and H_4L2 were synthesized following the Buchwald-Hartwig protocol developed in our laboratory for extended amino-carboxylate ligands.[19]

General procedure for synthesis of coordination polymers

The reagents were placed in a screw-capped Pyrex tube and dissolved in DMF by means of ultrasounds. The tube was then tightly closed and placed in a pre-heated oil bath and left

undisturbed until formation of crystals. The supernatant solution was then removed and the remaining crystals were plenty washed with DMF. To avoid degradation phenomena, the crystals were stored under DMF.

{[Zn₄O(L1)₃(DMF)₂](DMF)₄}ₙ·(DMF)ₓ (PUM*flex*1-Zn) or PUM*flex*1.1-Zn

$\{[Zn_4O(L1)_3(DMF)_2](DMF)_4\}_n \cdot (DMF)_x$ (PUM*flex*1-Zn) or PUM*flex*1.1-Zn

H₂L1 (212 mg, 0.5 mmol) and Zn(NO₃)₂·6H₂O (223 mg, 0.75 mmol) were dissolved in 5 ml of DMF in a 17 ml Pyrex tube. The solution was heated at 110°C for four days, at which time colourless plated crystals formed at the bottom of the vessel. Yield: 60% based on Zn. FTIR (cm⁻¹) for PUM*flex*1-Zn: 3301, 1661, 1595, 1384, 1325, 1176, 779. Elemental analysis was not reproducible due to partial loss of included solvent.

{[Zr₆O₄(OH)₈(L1)₄(H₂O)₂]ₙ}·(DMF)ₓ (PUM*flex*1-Zr)

$\{[Zr_6O_4(OH)_8(L1)_4(H_2O)_2]_n\} \cdot (DMF)_x$ (PUM*flex*1-Zr)

ZrCl₄ (55 mg, 0.24 mmol) was dissolved in 10 mL of DMF in a 17 mL Pyrex tube. Then 0.27 mL of TFA were added and the solution heated at 80°C for one hour. After slow cooling to room temperature, H₂L1 (50 mg, 0.12 mmol) was added and the sealed tube heated at 120°C for four days. White needle crystals formed. FTIR (cm⁻¹): 3240, 1663, 1596, 1366, 1330, 1179, 649. Elemental analysis was not reproducible owing to partial loss of solvents.

{[Cd(H₂L2)(DMF)₃](DMF)}ₙ (PUM*flex*2-Cd)

$\{[Cd(H_2L2)(DMF)_3](DMF)\}_n$ (PUM*flex*2-Cd)

H₄L2 (15 mg, 0.029 mmol) and Cd(NO₃)₂·4H₂O (22.6 mg, 0.073 mmol) were dissolved in 6 ml of DMF ina 10 mL Pyrex tube. The solution was heated at 80°C for four days, at which time brownish crystals formed. FTIR (cm⁻¹): 3282, 2929, 1642, 1539, 1365, 1099, 778, 660. Elemental analysis calcd. for C₄₀H₄₆CdN₆O₁₂ (found): C, 52.49 (52.45); H, 5.07 (4.99); N, 9.18 (9.09).

Crystallography

PUM*flex*1.1-Zn single crystal X-ray diffraction (SCXRD) data were collected on a D8 Bruker Venture diffractometer equipped with a kappa goniometer and an Oxford cryo-stream. Data collection were performed at 120 K under nitrogen flux. Microfocused MoKα radiation (λ = 0.71073 Å); Lorentz polarization and absorption correction were applied. Data were reprocessed using APEX v3 software. PUM*flex*1-Zn, PUM*flex*2-Cd and PUM*flex*1-Zr X-ray single crystal data collections (SCXRD) were performed at Elettra Sincrotrone (Trieste, Italy), beamline XRD1.[20] Crystals were directly picked from the soaking solution and data were collected at 100K by mean of an Oxford Cryostream system. The beamline spectra (produced by a NdBFe multipole wiggler) was monochromatized to 17.71KeV (0.700 Å) through a Si(111) double crystal monochromator and focused to obtain a beam size of 0.2 x 0.2 mm FWHM at the sample (photon flux 1012–1013 ph s⁻¹). Datasets were collected at 100 K (nitrogen stream supplied through an Oxford Cryostream 700) through the rotating crystal method. For triclinic crystals complete datasets were obtained merging two different data collections done on the same crystal, mounted with different orientations. Measurements were performed using a monochromatic wavelength of 0.700 Å on a Pilatus 2M hybrid-pixel area detector. The diffraction data were indexed and integrated using XDS.[21] Scaling was done using CCP4-Aimless code.[22,23] The structures were solved by the dual space algorithm implemented in the SHELXT code[24] in Olex2.[25] Fourier analysis and refinement were performed by the full-matrix least-squares methods based on F2 implemented in SHELXL-2014.[26] For all the structures, anisotropic displacement parameters were refined except for hydrogen atoms. PUM*flex*1-Zr presented poor resolution and merging statistics, due to the small dimensions of the crystal, and to its twinned condition. The best interpretation of diffraction data suggested a monoclinic *P21* space group, with centrosymmetric 45% twinning. The structure has been remarkably restrained to achieve convergence, and the architecture has been determined unambiguously.

PUM*flex*1-Zn, PUM*flex*1.1-Zn and PUM*flex*1-Zr showed large volumes of disordered solvent, which have been modelled with the MASK procedure implemented in Olex2. The residual density has been interpreted in terms of maximum potential number of DMF molecules, considering both the estimated number of residual electrons in the cavities (DMF accounts for 40 electrons), and the residual volume (DMF volume= 83Å3) with a packing efficiency of about 60%. For PUM*flex*2-Cd all the content of the pores has been modelled in terms of individual molecules.

Table 1 reports crystallographic data and details of structure refinements.

The analysis of topology and entanglement of the four structures, and the preparation of Figures 4-6 were accomplished by the use of ToposPro software.[18]

Conclusions

The two polydentate aminocarboxylate ligands used in this work combine the coordinating ability of the COO groups with the receptor ability of the N-H functions. The flexibility imparted by the N-H groups makes possible the blocking of different ligand conformation in the crystalline frameworks of the corresponding metal-assemblies. This was found in the case of H₂L1 with Zn(II), which led to two different polymorphic entangled frameworks, featured by different topology of the constituent 2D layers and different whole dimensionality. With Zr(IV) and Cd(II) only one phase was isolated. Unexpectedly, the tetracarboxylate ligand H₄L2 behaved as H₂L2²⁻ dianion, using only two COO functions to coordinate the metal making free the two remaining COOH groups to build a H-bond network involving neighbouring NH groups. In all cases the structural characterizations gave evidences of the good receptor capacity of the N-H groups towards guest, as evidenced by the recurrent N-H…O_DMF contacts found in the crystalline structures.

Topological analysis highlights the propensity of the used long flexible ligands to give rings which strongly influence the entanglement of the assembled extended motifs. Alongside to more common entanglement type, such as, 2-fold interpenetration/polythreading of 2D **sql** motifs with 2-loops or inclined polycatenation of **sql** layers, interestingly, a new

parallel polycatenated framework *via* Hopf link of **hcb** layers and a unique zirconium 1D motif of 2,8C1 topological type have been isolated and characterized. The host-guest properties of the isolated materials are currently under investigation in our laboratory.

Conflicts of interest

"There are no conflicts to declare".

Acknowledgements

Table 1. Crystal data and structure refinement for PUM*flex*1-Zn, PUM*flex*1.1-Zn, PUM*flex*2-Cd and PUM*flex*1-Zr

Identification code	PUM*flex*1-Zn	PUM*flex*1.1-Zn	PUM*flex*2-Cd	PUM*flex*1-Zr
Empirical formula	$C_{97.25}H_{99.25}N_{12.5}O_{18.97}Zn_4$	$C_{97}H_{96}N_{12}O_{19}Zn_4$	$C_{40}H_{46}CdN_6O_{12}$	$C_{104}H_{84}N_8O_{30}Zr_6$
Formula weight	2007.98	1995.33	915.23	2473.11
Temperature/K	100	100	100(2)	100
Crystal system	triclinic	monoclinic	orthorhombic	monoclinic
Space group	P-1	P2$_1$/n	Pbcn	P2$_1$
a/Å	15.2047(6)	11.5930(6)	12.4670(1)	19.551(1)
b/Å	18.4315(6)	45.238(2)	16.3496(1	24.348(2)
c/Å	28.608(1)	23.396(1)	21.3494(10)	19.579(1)
α/°	101.926(3)	90	90	90
β/°	96.440(3)	91.120(2)	90	98.16(2)
γ/°	98.138(3)	90	90	90
Volume/Å^3	7682.0(5)	12267.7(10)	4351.66(5)	9226(1)
Z	2	4	4	2
ρ_{calc}g/cm^3	0.868	1.080	1.397	0.890
μ/mm^{-1}	0.638	0.830	0.548	0.357
F(000)	2084.0	4136.0	1888.0	2488.0
Crystal size/mm^3	0.25 × 0.07 × 0.02	0.3 × 0.1 × 0.08	0.1 × 0.08 × 0.05	0.05 × 0.015 × 0.01
Radiation/Å	synchrotron (λ = 0.700)	MoKα (λ = 0.71073)	synchrotron (λ = 0.700)	synchrotron (λ = 0.700)
2Θ range for data collection/°	2.944 to 51.888	3.948 to 59.196	4.046 to 51.888	2.07 to 43.236
Reflections collected	98855	86045	55533	38188
Independent reflections	28924 R_{int} = 0.0709 R_{sigma} = 0.0677	33962 R_{int} = 0.0381 R_{sigma} = 0.0586	4457 R_{int} = 0.0407 R_{sigma} = 0.0133	20493 R_{int} = 0.2309 R_{sigma} = 0.3197
Data/restraints/parameters	28924/1331/1276	33962/480/1192	4457/332/316	20493/2450/1124
Goodness-of-fit on F^2	1.247	1.062	1.051	1.077
Final R indexes [I>=2σ (I)]	R_1 = 0.1061 wR_2 = 0.3141	R_1 = 0.0611 wR_2 = 0.1820	R_1 = 0.0596 wR_2 = 0.1896	R_1 = 0.1472 wR_2 = 0.3325
Final R indexes [all data]	R_1 = 0.1291 wR_2 = 0.3374	R_1 = 0.0839 wR_2 = 0.1985	R_1 = 0.0608 wR_2 = 0.1914	R_1 = 0.3108 wR_2 = 0.4094
Largest ΔF max/min / e Å^{-3}	2.08/-1.48	1.92/-0.81	2.31/-0.82	1.95/-1.03

Notes and references

1   Q. Yang, Z. Chen, J. Hu, Y. Hao, Y. Li, Q. Lu and H. Zheng, *Chem. Commun.*, 2013, **49**, 3585–3587.

2   M. H. Xie, Y. Wang, R. F. Li, P. Y. Dong, G. H. Hou, R. Shao, X. G. Xi, R. F. Guan and X. L. Yang, *Dalton Trans.*, 2018, **47**, 12406–12413.

3   Q. R. Fang, D. Q. Yuan, J. Sculley, J. R. Li, Z. B. Han and H. C. Zhou, *Inorg. Chem.*, 2010, **49**, 11637–11642.

4   D. Balestri, D. Capucci, N. Demitri, A. Bacchi and P. Pelagatti, *Materials*, 2017, **10**, 727-739.

5   Q. Yang, X. Chen, Z. Chen, Y. Hao, Y. Li, Q. Lu and H. Zheng, *Chem. Commun.*, 2012, **48**, 10016–10018.

6   L. Meng, K. Liu, S. Fu, L. Wang, C. Liang, G. Li, C. Li and Z.

ARTICLE

Journal Name

Shi, *J. Solid State Chem.*, 2018, **265**, 285–290.

7   D. Balestri, D. Costa, A. Bacchi, L. Carlucci and P. Pelagatti, *Polyhedron*, 2018, **153**, 278–285.

8   S. Canossa, P. Pelagatti and A. Bacchi, *Isr. J. Chem.*, 2018, **58**, 1131–1137.

9   B. Rees, L. Jenner and M. Yusupov, *Acta Crystallogr. Sect. D Biol. Crystallogr.*, 2005, **61**, 1299–1301.

10   D. Balestri, I. Bassanetti, S. Canossa, C. Gazzurelli, A. Bacchi, S. Bracco, A. Comotti and P. Pelagatti, *Cryst. Growth Des.*, 2018, **18**, 6824–6832.

11   Etter M.C., *Accounts Chem. Res.*, 1990, **23**, 120.

12   K. P. Lillerud, J. H. Cavka, C. Lamberti, N. Guillou, S. Bordiga, S. Jakobsen and U. Olsbye, *J. Am. Chem. Soc.*, 2008, **130**, 13850–13851.

13   J. Yang, J.-F. Ma, S. R. Batten, Chem. Commun. 2012, **48**, 7899-7912.

14   L. Carlucci, G. Ciani, D. M. Proserpio, T. G. Mitina and V. A. Blatov, *Chem. Rev*. 2014, **114**, 7557–7580.

15   E. V. Alexandrov, V. A. Blatov and D. M. Proserpio, CrystEngComm, 2017, **19**, 1993–2006.

16   E. V. Alexandrov, personal communication.

17   P. P.Bag, D. Wang, Z. Chen, R. Cao, *Chem. Commun.,* 2016, **52**, 3669-3672

18   V.A. Blatov, A.P. Shevchenko, D.M. Proserpio, Cryst. Growth Des. 2014, **14**, 3576-3586.

19   D. Balestri, A. Bacchi, P. Scilabra and P. Pelagatti, *Inorganica Chim. Acta*, 2018, **470**, 416-422.

20   A. Lausi, M. Polentarutti, S. Onesti, J.R. Plaisier, E. Busetto, G. Bais, L. Barba, A. Cassetta, G. Campi, D. Lamba, A. Pifferi, S.C. Mande, D.D. Sarma, S.M. Sharma, G. Paolucci *Eur. Phys. J. Plus*, 2015, 1–8.

21   W. Kabsch, *Acta Crystallogr. Sect. D Biol. Crystallogr.*, 2010, **66**, 125–132.

22   P. R. Evans and G. N. Murshudov, *Acta Crystallogr. Sect. D Biol. Crystallogr.*, 2013, **69**, 1204–1214.

23   M. D. Winn, C. C. Ballard, K. D. Cowtan, E. J. Dodson, P. Emsley, P. R. Evans, R. M. Keegan, E. B. Krissinel, A. G. W. Leslie, A. McCoy, S. J. McNicholas, G. N. Murshudov, N. S. Pannu, E. A. Potterton, H. R. Powell, R. J. Read, A. Vagin and K. S. Wilson, *Acta Crystallogr. Sect. D Biol. Crystallogr.*, 2011, **67**, 235–242.

24   G. M. Sheldrick, *Acta Crystallogr. Sect. A Found. Crystallogr.*, 2015, **71**, 3–8.

25   O. V. Dolomanov, L. J. Bourhis, R. J. Gildea, J. A. K. Howard and H. Puschmann, *J. Appl. Crystallogr.*, 2009, **42**, 339–341.

26   G. M. Sheldrick, *Acta Crystallogr. Sect. C Struct. Chem.*, 2015, **71**, 3–8.

Table of content entry

Flexible aminocarboxylate ligands have been used to construct coordination networks containing Zr, Zn and Cd featured by different dimensionality and topology